

DO THE NEARBY BHB STARS BELONG TO THE THICK DISK OR THE HALO?

T.D.KINMAN¹

NOAO, P.O.Box 26732, Tucson, Arizona 85726, USA

MORRISON, HEATHER, L.

Department of Astronomy, Case Western Reserve University, Cleveland, OH 44106, USA

BROWN, WARREN, R.

Smithsonian Astrophysical Observatory, 60 Garden St., Cambridge, MA 02138, USA

Accepted to AJ

ABSTRACT

We study the Milky Way region ($|Z| < 3.0$ kpc), where the thick disk and inner halo overlap, by using the kinematics of local blue horizontal branch (BHB) stars (within 1 kpc) and new samples of BHB stars and A-type stars from the *Century Survey*. We derive Galactic U , V & W velocities for these BHB and A-type star samples using proper motions from the *NOMAD* catalog. The mean velocities and the velocity dispersions of the BHB samples ($|Z| < 3$ kpc) are characteristic of the halo, while those of the *Century Survey* A-type stars are characteristic of the thick disk. There is no evidence from our samples that the BHB stars rotate with the thick disk in the region $|Z| < 3$ kpc. Nearly a third of the nearby local RR Lyrae stars have disk kinematics and are more metal-rich than $[\text{Fe}/\text{H}] \sim -1$. Only a few percent of the *Century Survey* BHB stars have these properties. Only one nearby BHB star (HD 130201) is likely to be such a disk star but selection based on high proper motions will have tended to exclude such stars from the local sample. The scale height derived from a sample of local RR Lyrae stars agrees with that of the *Century Survey* BHB stars. The local samples of BHB stars and metal-weak red giants are too incomplete for a similar comparison.

Subject headings: stars: horizontal branch, Galaxy: structure, Galaxy: halo

1. INTRODUCTION

The separation of the stellar thin disk, thick disk and halo populations near the Galactic plane is challenging because all three populations overlap spatially. The situation has become even more complex since Morrison et al. (2008) identified a new inner halo component with a vertical scale height comparable to that of the thick disk, which has, however, quite different kinematics. Inner halo stars have predominantly eccentric orbits, a much greater velocity dispersion than thick disk stars and no rotation. Thick disk stars, on the other hand, have kinematics that are dominated by rotation. Even so, one cannot unambiguously assign stars to the thick disk or halo using kinematics alone; metallicity provides an additional clue.

Almost all inner halo stars have $[\text{Fe}/\text{H}] < -0.8$, with a mean $[\text{Fe}/\text{H}]$ of -1.6 , whereas the mean $[\text{Fe}/\text{H}]$ of the thick disk is about -0.5 . The extent of the metal-weak tail of the thick disk is still uncertain. The first identifications of metal-weak thick disk stars were made using samples of red giants whose metallicity calibration was later shown to be unreliable (Norris et al., 1985; Morrison et al., 1990 and Twarog & Anthony-Twarog, 1994). Current studies of halo samples that have well-determined $[\text{Fe}/\text{H}]$ less than -1.0 (e.g. Morrison et al., 2008) show almost no disk stars, but they are based on surveys that avoid the Galactic plane. On the other hand, 35% of the local RR Lyrae stars have disk kinematics although

only a few of these disk RR Lyrae stars are more metal-poor than $[\text{Fe}/\text{H}] = -1.0$. This is discussed further in the Appendix.

BHB and RR Lyrae stars are among the most-used probes of the Galactic halo because both types of stars are effectively “standard candles”. Local BHB stars (within 1 kpc) have been reliably identified by high-resolution spectroscopy (Kinman et al. 2000; Behr 2003); their kinematics have not been discussed in detail, although their mean V_{LSR} is like that of the halo (Kinman et al. 2007 (Table 10)). Recently, Brown et al. (2008) in their *Century Survey Galactic Halo Project*, have identified 655 non-kinematically selected BHB stars. In this sample, those with $5 < |Z| < 9$ kpc show halo kinematics with a mean Galactic velocity (V_{LSR}) of ~ -220 km s^{-1} . In the region $2 < |Z| < 5.5$ kpc, however, Brown et al. found a gradient in this velocity of $dV_{LSR}/d|Z| = -28 \pm 3.4$ km s^{-1} . They also found a density scale height for the BHB stars of 1.26 ± 0.1 kpc and concluded that the BHB stars near the plane belong to the thick disk with a local space density of 104 ± 37 kpc^{-3} .

Brown et al. determined the mean Galactic velocity ($\langle V \rangle$) of their BHB stars from radial velocities *alone* since they considered that the existing proper motions were not accurate enough for them to get reliable U , V & W velocities for each star. While this is certainly true of the proper motions for the majority of the stars in their survey, it seems possible that the proper motions of their nearer stars (within 3 kpc) may be accurate enough to derive U , V & W velocities that could show whether these stars belong to the disk or to the halo. Our purpose

¹ The NOAO are operated by AURA, Inc. under cooperative agreement with the National Science Foundation.

is to examine this possibility.

2. GALACTIC KINEMATICS AND THE SEPARATION OF DISK FROM HALO BHB STARS

The Galactic U , V and W were derived from the proper motions, radial velocities and distances of each star using the program of Johnson & Soderblom (1987) that gives heliocentric velocities in a right-handed coordinate system that is positive towards the Galactic center, the direction of rotation and the NGP. These heliocentric velocities were converted to those relative to the local standard of rest (LSR) U_{LSR} , V_{LSR} and W_{LSR} using the solar motion $U_{\odot} = +10 \text{ km s}^{-1}$, $V_{\odot} = +5 \text{ km s}^{-1}$ and $W_{\odot} = +7 \text{ km s}^{-1}$ (Dehnen & Binney, 1998). The proper motions were taken from the *NOMAD* catalog (Zacharias et al. 2004a) using the *VizieR* access tool. This catalog lists the “best” proper motion available for a particular star from the following catalogs: Hipparcos (ESA, 1997), Tycho-2 (Hog et al. 2000), UCAC2 (Zacharias et al. 2004b) and USNO-B-1.0 (Monet et al. 2003). Most of the local sample have proper motions in the Hipparcos catalog and most of those in the *Century Survey* come from the UCAC2 catalog; only 17% of the proper motions of the *Century Survey* stars that are more distant than 2.75 kpc come from the less accurate USNO-B-1.0 catalog. The few stars in the *Century Survey* samples whose proper motions are not given in the *NOMAD* catalog were not used. The sources of the radial velocities and distances are discussed separately for each sample. All velocities are in km s^{-1} and we define the total space velocity (T) with respect to the LSR as $(V_{LSR}^2 + U_{LSR}^2 + W_{LSR}^2)^{0.5}$.

3. THE MEAN PROPERTIES OF THE SAMPLES.

Our local BHB sample (LBHB) consists of 27 stars within 1 kpc that were identified as BHB stars from high resolution spectra by Kinman et al. 2000 and Behr 2003; they give accurate radial velocities and $[\text{Fe}/\text{H}]$ for these stars. Their Johnson V & B magnitudes were corrected for interstellar extinction (Schlegel et al. 1998). Absolute magnitudes (M_v) were found from their $(B - V)_0$ color by the formula given by Preston et al. (1991) and their distances calculated. Table 1 presents the mean values of their Galactic velocities ($\langle U_{LSR} \rangle$, $\langle V_{LSR} \rangle$, $\langle W_{LSR} \rangle$), the dispersions in these velocities (σ_U , σ_V , σ_W), their mean total space velocity $\langle T \rangle$, their mean metallicity $\langle [\text{Fe}/\text{H}] \rangle$ and its dispersion $\sigma[\text{Fe}/\text{H}]$ and their mean height Z above the plane; the data for the individual stars of this LBHB sample are given in Table 2 [at end of manuscript].

Two samples (CBHB & CA) were taken from the *Century Survey* (Brown et al. 2008) using the classifications, distances, radial velocities and $[\text{Fe}/\text{H}]$ given in this paper with the *NOMAD* proper motions to compute the Galactic velocities of these stars. Sample CBHB consists of 82 BHB stars whose distances are less than 3.00 kpc. Sample CA contains 50 stars that were given spectral type A in the *Century Survey*; they are not BHB stars but presumed to be mostly stars of higher gravity. The mean J_0 magnitude of the stars in the CA sample is comparable with that of the BHB stars in sample CBHB; the errors in proper motions of the stars in these two samples should therefore be similar. The mean properties of the two samples of *Century Survey* stars are given in Table

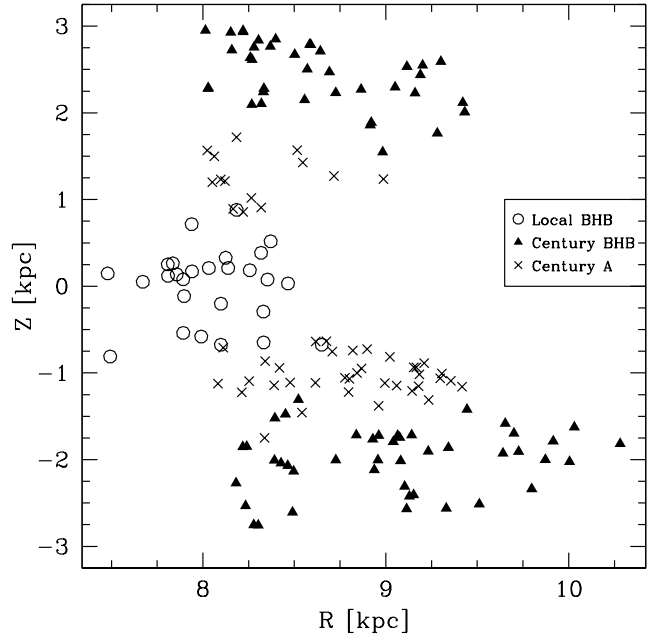


FIG. 1.— The Galactic spatial distributions of the local BHB sample (open circles), the Century BHB sample (filled triangles) and the Century A-type stars (crosses). R is the galactocentric distance and Z is the height above the plane. We assume that the Sun is located at $(R, Z) = (8, 0)$ kpc.

1 together with similar data for halo and thick disk samples for comparison; the data for the individual stars of the two samples of *Century Survey* stars are given in Table 3 [at end of manuscript]. The distances and velocities of the CBHB and CA samples were taken from Brown et al. (2008) where details are available from which their accuracies can be inferred. We note that the BHB absolute magnitudes of both the LBHB and CBHB samples are based on the cubic expression in $(B - V)$ given by Preston et al. (1991). In the case of the LBHB sample, the $(B - V)$ were directly observed colors while those used for the CBHB sample were derived from 2MASS photometry. At a very rough estimate, there might be a systematic difference of as much as 10% between the two distance scales. The mean error of the proper motions in each coordinate is $\pm 1.0 \text{ mas y}^{-1}$ for the LBHB sample, $\pm 3.1 \text{ mas y}^{-1}$ for the CBHB sample and $\pm 3.4 \text{ mas y}^{-1}$ for the CA sample.

The Galactic spatial distributions of these three samples are shown in Fig. 1. If significant systematic errors were present in the *NOMAD* proper motions, we would expect them to produce non-zero values in the mean U and W velocities since there is no evidence that a major halo stream passes through the solar neighborhood (c.f. Seabroke et al. 2008). The measured values of $\langle U \rangle$ and $\langle W \rangle$ are $+10 \pm 24$ and $-04 \pm 18 \text{ km s}^{-1}$ for the LBHB and -14 ± 14 and $+13 \pm 09 \text{ km s}^{-1}$ for the CBHB sample respectively. We conclude that the proper motions do not contain a systematic error which would produce an error in $\langle U \rangle$ and $\langle W \rangle$ that is as large as 20 km s^{-1} . Errors in the proper motions of the CBHB sample will have their greatest effect on the space velocities U and V for stars at the North Galactic Pole. In this location an error of 1.0 mas y^{-1} will produce a maximum error of 20 km s^{-1} in either U or V for a star at a distance of

TABLE 1
COMPARISON OF THE GALACTIC KINEMATICS OF THE VARIOUS SAMPLES.

Sample ^a	N ^b	$\langle U_{LSR} \rangle$	$\langle V_{LSR} \rangle$	$\langle W_{LSR} \rangle$	σ_U ^c	σ_V ^c	σ_W ^c	$\langle T \rangle$	$\langle [\text{Fe}/\text{H}] \rangle$ ^d	$\sigma[\text{Fe}/\text{H}]$ ^e	$ Z $ ^f
LBHB	27	+10±24	-207±15	-04±18	121±16	077±10	090±12	260±13	-1.67±0.09	0.43±0.06	0.34
CBHB	82	-14±14	-212±12	+13±09	121±10	106±08	078± 6	266±12	-1.63±0.06	0.50±0.04	2.20
CA	50	+28±12	-043±11	-00±07	086±09	074±07	047± 5	113±12	-0.52±0.08	0.42±0.08	1.10
MWRG	81	155±07	109±05	101±05	...	-1.92±0.05	...	0.65
HALO 2	78	-17±16	-187±12	-05±11	141±11	106±09	094±08
THICK DISK	-046±05	...	063±06	039±04	039±04	...	-0.48±0.05	0.32±0.03	...

^a (LBHB) Local BHB stars, (CBHB) *Century Survey* BHB stars within 3.00 kpc (CA) *Century Survey* stars of spectral type A. MWRG is a local sample of metal-weak red giants with $[\text{Fe}/\text{H}] < -1.0$ and that lie within 1 kpc (Kepley et al., 2007); HALO 2 is a local sample of halo stars with $[\text{Fe}/\text{H}] \leq -2.2$ (Chiba & Beers, 2000); the THICK DISK sample is from Soubiran et al., 2003.

^b Number of stars in sample.

^c Dispersions of U , V & W in km/s.

^d Mean $[\text{Fe}/\text{H}]$ of sample.

^e Dispersion in $[\text{Fe}/\text{H}]$ of sample.

^f Mean height of sample above Galactic plane (kpc).

3 kpc. We therefore consider that the likely systematic error in these proper motions is not likely to produce a systematic error in V that is greater than 20 km s^{-1} . In support of this conclusion, we note that the V_{LSR} that we find for the LBHB and CBHB samples agree with that of the HALO2 sample within this error.

We see that the $\langle V_{LSR} \rangle$ of the BHB stars in the LBHB and the *Century Survey* CBHB samples as well as their dispersions in U , V & W are similar to those of the halo samples in Table 1. The kinematics of sample CA, on the other hand, are similar to those of the thick disk sample (Soubiran et al. 2003) and significantly different from those of the *Century Survey* BHB samples. The Galactic velocities of these BHB stars at $|Z|$ of 0.34 & 2.20 kpc show that, on average, they have halo rather than disk kinematics.

3.1. The Effects of Selection on the Samples.

The *Century Survey* stars were selected photometrically and therefore have no kinematic bias. A comparison of the classification of the *Century Survey* stars with previous classifications of BHB stars at the North Galactic Pole (Kinman et al., 2008) shows very good agreement and gives confidence that the *Century Survey* classifications are largely correct ². The local (LBHB) sample may have some kinematic bias because many of its stars were selected because of their high proper motions³. The bias cannot be very large, however, because (to a first order) the local and *Century Survey* BHB stars have similar kinematics (Table 1).

To examine the possible bias of the 27-star LBHB sample in more detail, we used a sample of 75 first-ascent halo red giants which were selected without kinematic bias. These stars all have $[\text{Fe}/\text{H}] < -1.0$, distance less than 1 kpc and are a subset of the local halo sample of Morrison et al. (2008). We randomly selected 1000 sub-samples of

² Seven of the BHB stars in Table 3, CHSS 833, 196, 2103, 2152, 2323, 2353 and 2372 have been previously classified as BHB stars; only one, CHSS 2349 (HZ 31) has been classified differently (Greenstein & Sargent, 1974; Hill et al., 1982.)

³ In Table 2, an asterisk following the star's HD or BD number shows that it was selected by its color alone. The remaining stars were selected by color from a proper-motion limited sample.

size 27 from this sample and examined how often these had the same kinematic parameters as the LBHB sample. If the LBHB sample has significant kinematic selection effects, its parameters ($\langle V \rangle$, σ_U , σ_V and σ_W) should be different from those of the red giant sample. They should therefore appear only rarely in the 1000 sub-samples. In fact, the actual values of $\langle V \rangle$, σ_U and σ_W appeared quite often; thus, these values appeared in 61%, 8% and 44% of the subsamples respectively. Only the value of σ_V (77 km s^{-1} in the LBHB sample) appeared just 1.5 % of the time in the 1000 sub-samples. This shows that the LBHB sample is only significantly different in σ_V (and this at a fairly low significance level) from the unbiased red giant sample. This difference is in the expected sense if the local BHB sample lacks stars with low proper motions, but it is clearly not a strong effect. The question of selection on local halo samples is discussed further in the Appendix.

We made a similar comparison between the local red giant sample (now with distances less than 2.5 kpc) and the 82-star *Century Survey* BHB sample. In this case, we found no significant differences in the mean V velocity, σ_U , σ_V , and σ_W when 1000 sub-samples of 82 stars from the red giant sample were compared with the BHB sample. These values or smaller ones occurred 8%, 10%, 33% and 9% of the time. The median $|Z|$ of the local red giant sample is 0.65 kpc and so it is closer to the plane than the *Century Survey* BHB sample and some small difference in kinematics might have been expected (Morrison et al. 2008), but none was found.

3.2. How many Thick Disk BHB stars could there be?

The earliest systematic characterizations of stellar populations (e.g. Oort, 1958) assumed that the older populations were *smoothly* distributed. This assumption is still implicit in much work on the disk populations which are commonly defined by a scale heights, scale lengths and velocity dispersions in orthogonal coordinates. Recent research on the halo, however, has shifted very largely to studies of how it departs from a smooth distribution, either as overdensities or the clumping in the distribution of kinematic quantities that are adiabatic invariants.

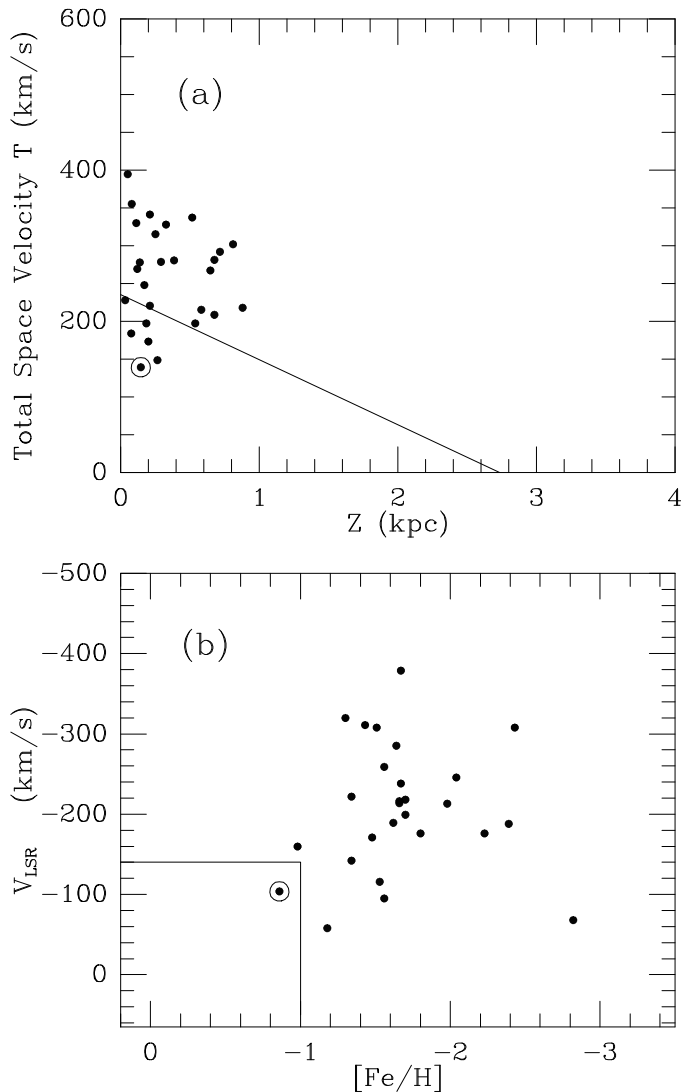


FIG. 2.— The local BHB Sample LBHB. The significance of the lines is described in Sec. 3.2. The star (HD 130201) whose Bayesian probability of belonging to the halo is less than 0.5 (i.e. a likely disk star) is shown encircled.

The latter approach is only possible for those relatively nearby stars that have well-determined distances, radial velocities and proper motions (Helmi et al., 1999, Kepley et al., 2007, Morrison et al., 2008). For the present, when we characterize the halo by parameters (such as the scale height, and velocity dispersions) that are appropriate for smooth distributions, we must remember that the validity of these parameters may be limited. The incompleteness of samples will also limit the conclusions that drawn about these parameters. With these *caveats* we use three criteria for distinguishing disk from halo stars:

(1) Martin & Morrison (1998) showed that in a plot of the total space velocity (T) against $|Z|$ (the height above the plane), the thick-disk RR Lyrae stars lie below the line which has $T = 235$ km/s at $Z = 0$ kpc and $T = 0$ km/s at $Z = 2.73$ kpc. We give this plot for the local BHB sample sample, the *Century Survey* BHB sample and the *Century Survey* A-type star sample in Figs 2(a), 3(a) & 4(a) respectively. On this criterion, six (22%) of the LBHB sample are disk stars but only one (1%) of the CBHB sample. On the other hand, the majority (76%) of the CA sample (non-BHB A-type stars) belong to the

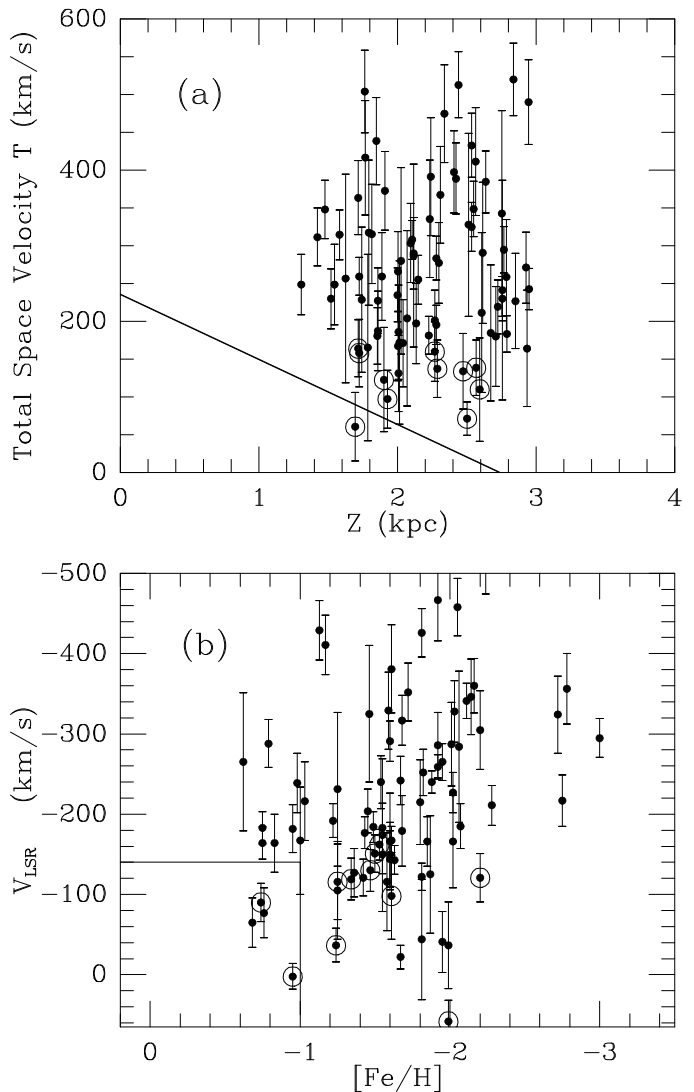


FIG. 3.— The *Century Survey* BHB sample CBHB. The significance of the lines is described in Sec. 3.2. Stars whose Bayesian probability of belonging to the halo is less than 0.5 (i.e. likely disk stars) are shown encircled.

disk.

(2) Layden et al, (1996) used three different criteria to define disk stars. These were also used by Dambis & Rastorguev (2001) who preferred their Disk-2 criterion because it gave the least contamination by halo stars. We give reasons for agreeing with this conclusion in the Appendix (A.2). This criterion defines disk stars as having $[Fe/H] \geq -1.0$ and $V_{\theta} > +80$ km s $^{-1}$ ($V_{LSR} \sim > -140$ km s $^{-1}$). These limits are shown as the box in the V_{LSR} vs. $[Fe/H]$ plots for the local BHB sample, the *Century Survey* BHB sample and the *Century Survey* A-type star sample in Figs 2(b), 3(b) & 4(b) respectively. On this criterion, only one of the LBHB sample is a thick disk member and only four (5%) of the *Century Survey* CBHB sample belongs to the thick disk, but 36 (72%) of the CA sample are disk stars.

(3) Venn et al. (2004) calculated the Bayesian probabilities P_{thin} , P_{thick} , P_{halo} that a star belongs to the thin disk, thick disk and halo respectively from its fit to the corresponding thin disk, thick disk & halo galac-

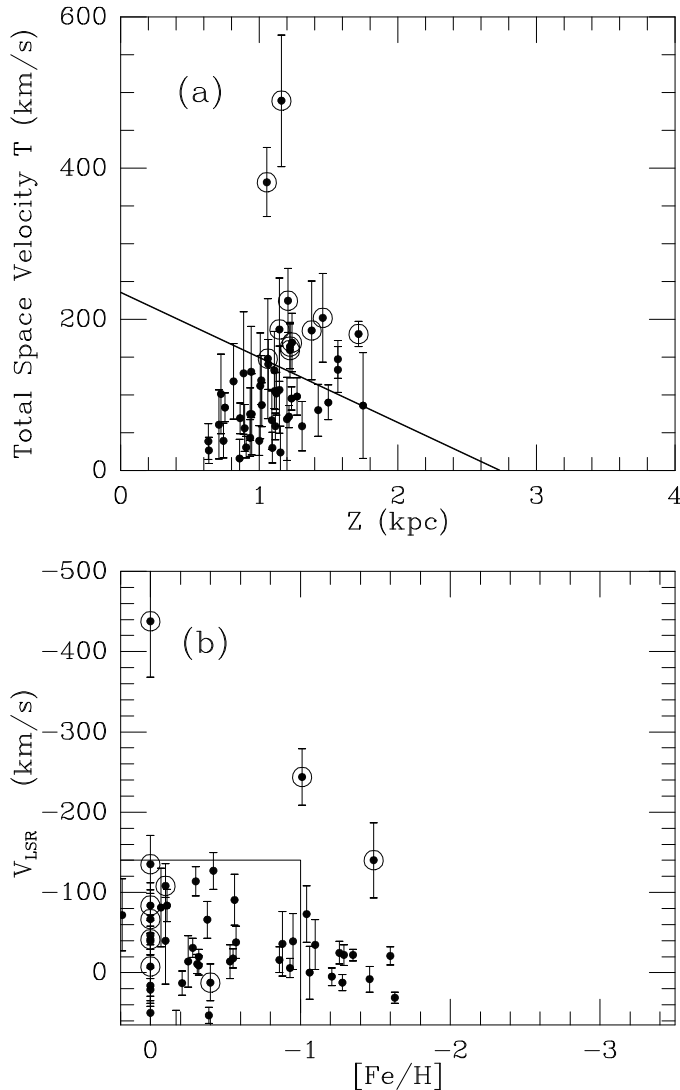


FIG. 4.— The *Century Survey* A-type star sample CA. The significance of the lines is described in Sec. 3.2. Stars whose Bayesian probability of belonging to the halo is more than 0.5 (i.e. likely halo stars) are shown encircled.

tic Gaussian velocity ellipsoid components⁴. We determined these Bayesian probabilities (normalized so that $P_{thin} + P_{thick} + P_{halo}$ equals unity); they are given in Tables 2 and 3 [at end of manuscript]. We used the same priors as Venn et al. for the thin disk and thick disk but used the velocity ellipsoid of the red giant sample (Morrison et al., 2008) for the halo. Stars that have $P_{halo} \leq 0.50$ are shown encircled in Figs. 2 and 3. Stars with $P_{halo} \geq 0.50$ are shown encircled in Fig. 4.

The mean probability P_{disk} ($P_{thin} + P_{thick}$) that a star belongs to the disk and not the halo is 0.045 ± 0.023 , 0.133 ± 0.028 and 0.750 ± 0.052 for the local BHB, *Century Survey* BHB and *Century Survey* A-type non-BHB stars respectively. Only one star (HD 130201) in the local BHB sample has both the kinematics and $[Fe/H]$ to make it likely to be a disk star. In the *Century Survey*, there are ten BHB stars that have both $P_{disk} > 0.50$ but only two of these have $[Fe/H] > -1.0$. In the Appendix

⁴ Thin Disk (Dehnen & Binney, 1998); Thick Disk (Soubiran et al., 2003) and Halo (Chiba & Beers, 2000). Similar estimations of such Bayesian probabilities have been given by Mishenina et al., 2004 and Reddy et al., 2006.

(A.2), we show that the use of Bayesian probabilities to select *disk* RR Lyrae stars leads to the inclusion of metal-weak stars with increasing height above the plane. Thus we need a metallicity restriction if we are to define the disk in terms of a homogeneous population. It is particularly needed for samples such as the *Century Survey* that are well outside the plane. If we take into account the formal uncertainties of the *Century Survey* $[Fe/H]$ (± 0.25 dex), we conclude that not more than two or three of the CBHB sample are likely to belong to the disk if it defined by the Disk-2 criterion of Layden et al. (1996). An estimate of an upper limit to the fraction disk stars in the CBHB sample is discussed in the Appendix.

There are eleven A-type stars in the *Century Survey* CA sample whose P_{halo} exceeds 0.50. Nine of these, however, have $[Fe/H] > -0.5$ and so are most unlikely to belong to the halo. Also, as in the case of the *Century Survey* CBHB sample, there is a metal-weak tail to stars whose P_{disk} exceeds 0.50. Brown et al. (2008) estimated the distances of their A-type stars assuming that they have the absolute magnitudes of globular cluster blue stragglers of the same $(B-V)_0$ and $[Fe/H]$. The difficulty of assigning absolute magnitudes to this probably heterogeneous class of stars may well have led to less certain kinematics than for the *Century Survey* BHB stars. We presume that nearly all the stars in the CA sample are higher-gravity A-type stars (including blue stragglers) of the thick disk and the balance of the evidence agrees with this.

4. SUMMARY

We used *NOMAD* proper motions for 82 BHB stars from the *Century Survey* that are nearer than 3 kpc to get Galactic velocities U, V & W whose systematic errors probably do not exceed 20 km s^{-1} . The mean U, V & W and corresponding velocity dispersions of these *Century Survey* BHB stars (CBHB sample) ($\langle |Z| \rangle > 2.20$ kpc) are very similar to those of a local (LBHB) sample of BHB stars ($\langle |Z| \rangle > 0.34$ kpc) and of other local halo stars such as the red giant (MWRG) sample of Morrison et al. (2008). In a detailed comparison, the CBHB sample shows no significant difference from this MWRG sample, but the LBHB sample has a (99% significant) smaller velocity dispersion (σ_V). We show (Appendix A3) that this is probably caused by a lack of low proper motion stars among the more distant stars in the LBHB sample.

We discuss several criteria for distinguishing between disk and halo stars. The *most practical*, currently, is the Disk-2 criterion of Layden et al. (1966); this excludes disk membership for stars with $[Fe/H] < -1.0$. Using this, only two or three of the CBHB sample are likely to belong to the disk and only one (HD 130201) of the LBHB sample. The expected distribution of proper motions in a local *disk* sample is such, however, that very few disk stars would be expected in the current LBHB sample. If we had not put any metallicity restriction on disk membership, 11% of our CBHB sample might belong to the disk. We take this to be an upper limit to number of disk stars in this sample. This upper limit for the percentage of disk stars in the BHB sample is much lower than the 35% found in the sample of local RR Lyrae stars (99.9% significance). A sample of 50 non-BHB stars that are classified as A-type in the *Century*

Survey ($\langle |Z| \rangle > 1.10$ kpc), on the other hand, were found to be largely disk stars.

The cumulative number of stars within a given distance for a population of stars that has the scale height (1.26 kpc) of the *Century Survey* BHB stars is compared with those in the LBHB sample, a local RR Lyrae sample and the MWRG sample. The RR Lyraes within 850 to 900 pc show a similar scale height to the CBHB sample in agreement with previous determinations (Amrose & McKay, 2001; Maintz & de Boer, 2005). The LBHB and MWRG samples show significant incompleteness beyond 350 and 250 pc respectively so that only limited comparisons with them are possible. All three of these local samples show incompleteness at lower galactic latitudes when compared with the numbers expected with the scale height given by the *Century Survey*.

We therefore conclude that the CBHB stars, like the RR Lyrae stars, form a quite flattened system (like the thick disk) near the Galactic plane *but that most of these CBHB stars belong to the inner halo and are not disk stars*.

We are very grateful to Dr Mike Irwin for providing us with his program for calculating population probabilities and Dr Sabine Moehler, Dr Sofia Feltzing and an anonymous referee for helpful comments. This research has made use of the VizieR catalogue access tool, CDC, Strasbourg, France.

5. APPENDIX

5.1. *Comments on the completeness and composition of local samples.*

Our samples consist of (a) BHB stars, (b) RR Lyrae stars and (c) metal-weak red giant stars that are within 1 kpc. The BHB sample (LBHB) is that in Table 2 [at end of manuscript] where an asterisk after the ID shows that the star was identified as a BHB star by its color alone; the remainder were identified by color from among stars with proper motions exceeding 50 mas yr^{-1} . The RR Lyrae sample was taken from a recent compilation by Maintz and de Boer (2005) of 217 RR Lyrae stars for which distances and radial velocities were taken from the literature and proper motions from the Hipparcos and Tycho-2 catalogues; they used these data to derive the galactic orbits for these stars. We classified these RR Lyrae stars as *disk* or *halo* using the Bayesian probabilities described in Sec. 3.2. The metal-weak red giant (MWRG) sample, taken from Kepley et al. (2007), is given as a halo sample in Table 1. We note that four out of the ten MWRG stars that are within 300 parsecs⁵ were originally observed because of their high proper motions; little such kinematic bias is expected in the selection of the more distant MWRG because they were discovered from objective prism spectra. Table 4 summarizes the mean properties of these samples. The *disk* RR Lyrae sample is not only significantly more metal-rich than the halo RR Lyrae sample but also has a significantly different mean pulsation period.

5.2. *How well can we identify disk RR Lyrae stars?*

Maintz and de Boer (2005) define *disk* RR Lyrae stars as having a galactic rotation (Θ) greater than 100 km s^{-1} , an orbital eccentricity less than 0.4 and a normalized z-extent less than 0.4 kpc. All 18 of the *disk* RR Lyrae stars that we identified by Bayesian probabilities would also be identified as disk stars by these criteria except for SW Dra (which has an orbital eccentricity of 0.42). Among 50 RR Lyrae stars that belong to the disk according to the Maintz and de Boer criteria, only two (v675 Sgr and RV Sex) have Bayesian probabilities that would assign them to the halo. Close to the galactic plane, therefore, the Bayesian probabilities seem to give an adequate description of the kinematic properties. If we consider the RR Lyrae stars in the Maintz & de Boer catalog that lie more than 1 kpc from the plane, we find 11 stars whose Bayesian probabilities assign them to the disk. They have $[\text{Fe}/\text{H}]$ in the range -0.45 to -2.23 , a mean $[\text{Fe}/\text{H}]$ of -1.30 ± 0.17 and a mean period of 0.538 ± 0.024 . This sample of *disk* RR Lyrae stars ($\langle |Z| \rangle = 1.37 \pm 0.11 \text{ kpc}$) is significantly different from those with $|Z| < 1.0$ (Table 4). This is shown in the V -amplitude *vs.* log period plot of Fig. 7 for the type *ab* RR Lyraes selected as disk members by their Bayesian probabilities. The curve is that for Oo I variables in the globular cluster M3 ($[\text{Fe}/\text{H}] = -1.5$) from Cacciari et al., (2005) who show (in their Fig. 4) that the type *ab* RR Lyrae stars in halo globular clusters ($[\text{Fe}/\text{H}] < -1.0$) either scatter around this line or lie to the right of it. RR Lyrae stars in metal-rich bulge globular clusters lie well to the right in this diagram and only the field metal-

⁵ HD 6755, HD 25532, HD 44007 & HD 175305 (Roman, 1955)

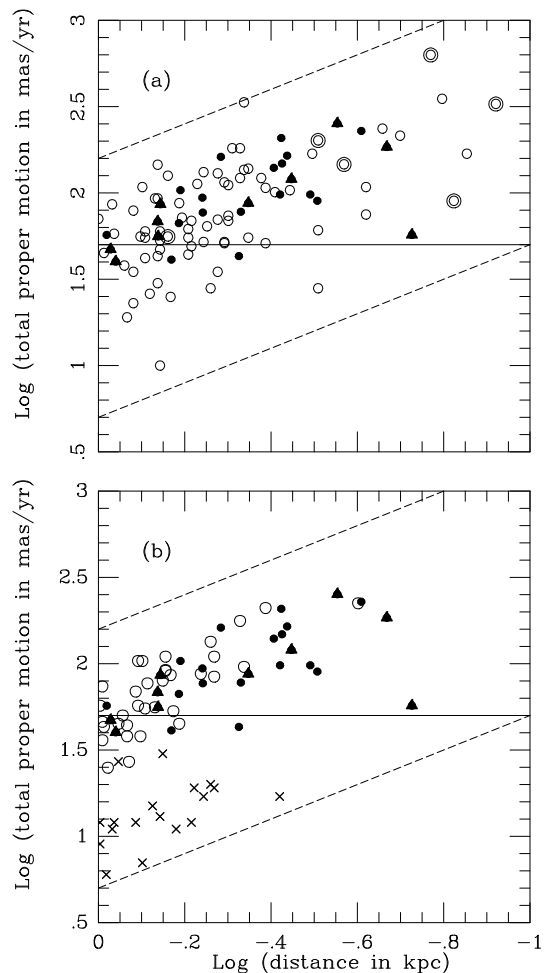


FIG. 5.— The ordinate is the log of the total proper motion (mas yr^{-1}) and the abscissa is the log of the distance in kpc. In both (a) and (b) the local sample of BHB stars is shown by filled circles if the stars were found in a proper-motion selected sample and by filled triangles if they were found by their colors alone. In (a), the metal-poor red giant sample from Kepley et al. (2007) is shown by open circles. A double circle indicates that the stars were identified in a proper motion selected sample. In (b), the *halo* RR Lyrae stars are shown by open circles and the *disk* RR Lyrae stars by crosses. The significance of the lines is given in the Appendix (A.3).

rich disk RR Lyrae stars lie *systematically* to the left of this curve (Pritzl et al., 2000). The local *disk* RR Lyrae stars that have $|Z| < 1.0 \text{ kpc}$ that lie to the left of the M3 curve in this diagram are all more metal rich than $[\text{Fe}/\text{H}] = -1.16$ and it seems reasonable to assume that they comprise a more or less homogeneous population. This is not true of the sample that is more distant from the plane. We conclude that we should only use the small sample of stars near the plane to define *disk* HB stars. These considerations suggest that the Disk-2 definition (Layden et al., 1996) that excludes stars more metal-weak than $[\text{Fe}/\text{H}] = -1.0$ is currently the best practical (if somewhat conservative) definition; this agrees with the conclusion of Dambis & Rastorguev (2001).

5.3. *Proper motions as a function of distance*

In Fig. 5 we compare the proper motions as a function of distance for (a) the BHB and MWRG samples and (b) the BHB and the RR Lyrae samples. The solid horizontal line in these log – log plots corresponds to a proper motion of 50 mas yr^{-1} (the limit of the survey of Stet-

son (1991)). For a given velocity, the proper motion will decrease inversely with the distance. Consequently, in a log-log plot of the proper motion against the distance, the points should scatter in a band of unit slope. It is seen that the data lie in such bands (indicated by dashed lines) in Fig. 5. Any systematic differences between the distance scales of our different samples would result in a horizontal shift of one sample with respect to another on this plot. Such differences appear to be small in the case of the *halo* samples. The proper motions of the largest sample (the MWRG) in Fig. 5(a) are all greater than 50 mas y^{-1} for stars within 0.25 kpc. The selection of BHB stars by their proper motions will therefore miss few if any stars closer than this distance but could miss perhaps half the stars at a distance of 0.8 kpc. The distances of the *disk* RR Lyrae stars are less certain than those of their *halo* counterparts. If we adopted the absolute magnitude $M_v = +1.11$ derived from statistical parallaxes by Dambis & Rastorguev (2001), the log D of these stars would be reduced by ~ 0.1 . Even so, a population with the kinematics of the *disk* RR Lyraes would have few stars with proper motions $> 50 \text{ mas y}^{-1}$ unless their local space density is very much larger than that of the RR Lyraes.

5.4. A comparison with the predictions of the *Century Survey*.

Brown et al. (2008) showed that the *Century Survey* BHB stars with $|Z| < 4 \text{ kpc}$ fitted an exponential disk with a scale height of $1.26 \pm 0.1 \text{ kpc}$ and a local space density of $104 \pm 37 \text{ stars kpc}^{-3}$. We computed the number (n) of BHB stars that would be found within a distance (D) according to this model and compared it with the number (N) that are actually observed. We show $\log n - \log N$ as a function of D in Fig. 6(a)(b)(c) for our BHB, RR Lyrae and MWRG samples respectively. We would expect that $\log n - \log N$ would be constant for a given type of star if the model is applicable. The RR Lyrae stars show little trend of $\log n - \log N$ with distance which suggests that they have the same scale-height as the *Century Survey* BHB stars. Amrose & McKay (2001) discussed 186 type *ab* RR Lyrae stars that were found in the *Robotic Optical Transient Search Experiment* (ROTSE) survey and found an exponential distribution which was consistent with scale heights between 0.58 and 1.50 kpc. Maintz & de Boer found a scale height that is 1.25 to 1.30 kpc for the RR Lyraes near the plane. We take this as evidence that both the *Century Survey* BHB stars and RR Lyrae stars have similar scale heights. In the case of the BHB and MWRG samples, $\log n - \log N$ is initially constant but then decreases with increasing distance. We take this as evidence that both these samples show *distance-dependent incompleteness*. The alternative explanation would be that they have improbably small scale heights. The space densities in Table 3 were calculated using only the range of distance over which $\log n - \log N$ was considered constant for each sample. The errors of these space densities were calculated by Poisson statistics from the number of stars used to derive the space densities; they do not take incompleteness into account.

We calculated the ratio of the number of stars that would be expected to be observed at galactic latitudes (b) greater than 30° to the expected number at latitudes less than 30° . This ratio is shown as a function of distance

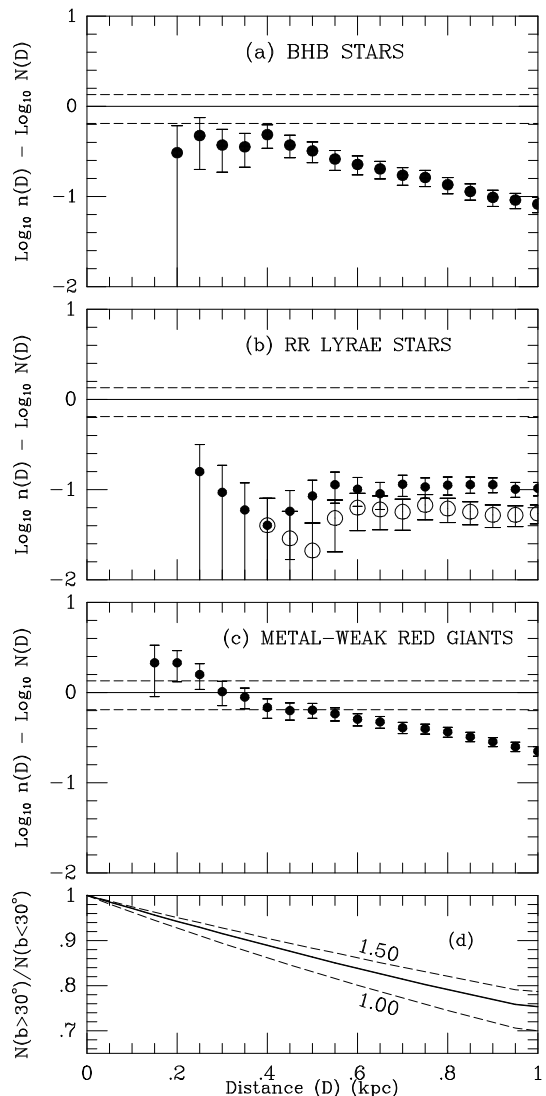


FIG. 6.— The ordinate is difference between $\log n(D)$ and $\log N(D)$ where $n(D)$ is the number of BHB stars within a distance D that is predicted by the *Century Survey* model and $N(D)$ is the observed number of stars. The abscissa is the distance D in kpc. The plots in (a), (b) and (c) are for the BHB stars, RR Lyrae star and metal-weak red giants respectively. The filled and open circles in (b) refer to *halo* and *disk* RR Lyrae stars respectively. The error bars were calculated from Poisson statistics. The horizontal dashed lines indicate the uncertainty in the local density that is predicted by the *Century Survey* model. Fig. 5 (d) is described in the text.

in Fig. 6(d) for scale heights of 1.26 kpc (full line) and 1.00 and 1.50 kpc (dashed lines). The observed numbers are given in Table 3 [at end of manuscript] and generally show fewer than the expected number of lower latitude stars; this is not at all unexpected since the crowding and increased extinction at lower latitudes will make surveys less effective. The problem is particularly severe for the MWRG sample because objective prism surveys require relatively uncrowded fields.

5.5. The distribution of $[\text{Fe}/\text{H}]$ in the different local halo samples.

The distributions of $[\text{Fe}/\text{H}]$ in the BHB and *halo* RR Lyrae samples are sufficiently similar (Table 3 & Fig.6) that we can combine them and the resulting distribution has 32 stars in the range $-1.40 < [\text{Fe}/\text{H}] < -1.80$ and 10 that are more metal-poor than $[\text{Fe}/\text{H}] = -1.80$. The cor-

TABLE 4
COMPARISON OF HALO SAMPLES WITHIN 1 kpc.

Type ^a	N ^b	N _{high} ^c	N _{low} ^d	Range in [Fe/H]	<[Fe/H]>	<[Z]>	<Ecc.> ^e	<P _{ab} > ^f	ρ(d) ^g	d ^h
RR(D)	18	7	11	-0.07 to -1.34	-0.62±0.11	0.31±0.05	0.17±0.03	0.46±0.02	6±2	0.85
RR(H)	34	20	14	-0.71 to -2.43	-1.52±0.06	0.42±0.04	0.67±0.03	0.55±0.02	12±1	0.90
LBHB	27	18	19	-0.86 to -2.43	-1.67±0.08	0.34±0.05	37±15	0.35
MWRG	81	52	29	-1.09 to -3.09	-1.92±0.05	0.36±0.03	190±78	0.20

^a RR(D) Disk RR Lyrae stars; RR(H) Halo RR Lyrae stars; LBHB BHB stars as in Table 1; MWRG Metal-weak red giant (same as HALO1 in Table 1).

^b Number of stars in sample.

^c Number of stars with galactic latitude > 30°

^d Number of stars with galactic latitude < 30°

^e Mean eccentricity of Galactic orbit from Maintz & de Boer (2007)

^f Mean period assuming the “fundamentalized” period of type *c* RR Lyraes is 1.342 times their actual period.

^g Local space density (stars per cubic kpc).

^h distance in kpc within which ρ(d) was estimated.

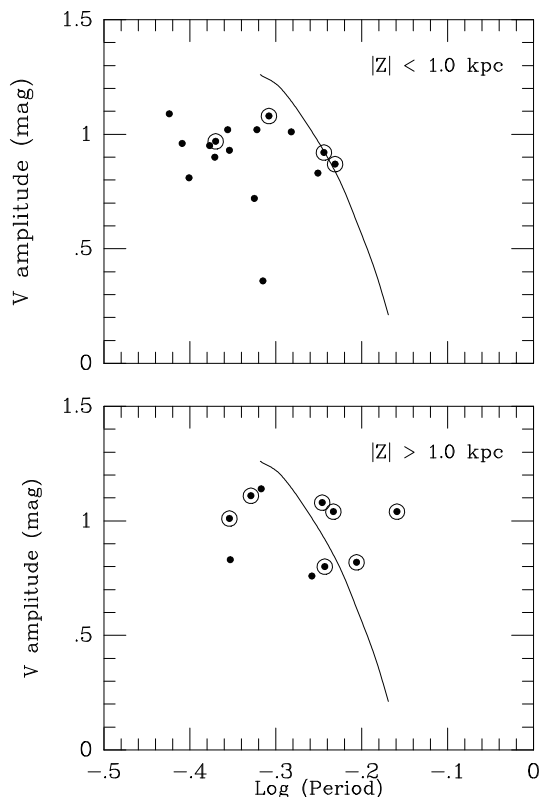


FIG. 7.— V-amplitude vs. log(Period) for *disk* type-*ab* RR Lyrae stars selected by their Bayesian probabilities for (above) stars with $|Z| < 1$ kpc and (below) stars with $|Z| > 1$ kpc. Stars with $[Fe/H] < -1.0$ are shown encircled. The curve is the relation for the globular cluster M3 (Cacciari et al., 2005).

responding numbers for the MWRG sample are 26 and 44. These distributions differ with a greater than 99.9% significance. We conclude that either (a) the MWRG sample is deficient relative to the combined HB sample in the range $-1.40 < [Fe/H] < -1.80$, or (b) the combined HB sample is very deficient in stars with $[Fe/H] < -1.8$, or (c) there are systematic differences between the metallicity scales or (d) a combination of all of these. A further investigation is desirable but beyond the scope of this paper.

5.6. The future discovery of disk BHB stars.

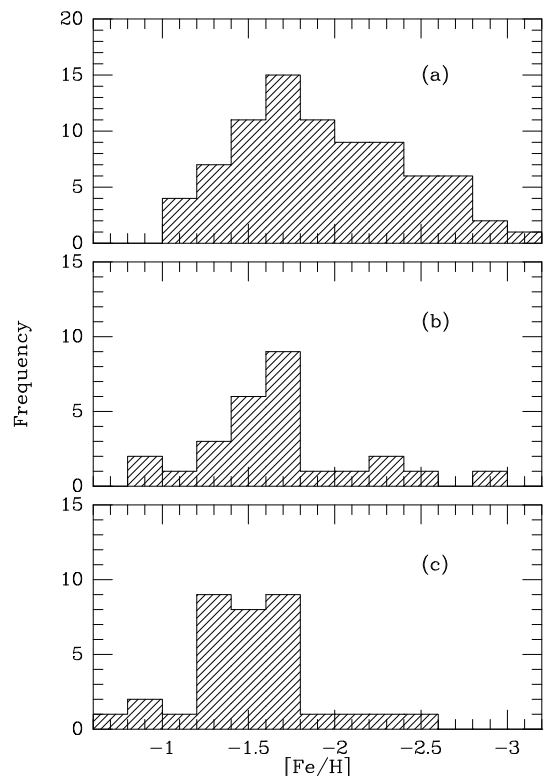


FIG. 8.— The distribution of $[Fe/H]$ among different samples of halo stars within 1 kpc. (a) MWRG sample; (b) BHB sample and (c) *halo* RR Lyrae sample.

HD 130201 is the only likely disk BHB candidate. It was recognized as a BHB star by Stetson (1991) from a proper-motion selected sample. It is an E-region photometric standard (Menzies, et al., 1989) and, in principle could have been recognized as a BHB star from its *UBV* colors. The extinction is sufficiently uncertain at this star’s galactic latitude ($+12.5^\circ$), however, that a definite classification would have been difficult. Stetson, (1991) and Brown et al., (2008) have pointed out that colors that would allow the identification of BHB stars at high galactic latitudes or among high proper motion samples may give ambiguous results at lower latitudes where there are large numbers Population I stars. The best hope for discovering *disk* BHB stars is therefore at higher latitudes where the identification process is more effective and the

expected numbers are not very much less than those at lower latitudes.

5.7. Postscript on the Metal-Weak Thick Disk.

In this paper we have assumed that there are no Thick Disk stars with $[\text{Fe}/\text{H}] < -1.0$. In other words that there is no metal-weak Thick Disk (MWTD). While Chiba and Beers (2000) report a contribution of 30% of the MWTD in the abundance range of $-1.7 < [\text{Fe}/\text{H}] < -1.0$,⁶ it has been known for some time (e.g. Morrison et al. 1990) that this fraction is much lower for the RR Lyrae variables. Ivezić et al. (2008) find $\sim 15\%$ contribution for the MWTD and none more metal-poor than $[\text{Fe}/\text{H}] = -1.5$, but this result contains no correction for the accuracy of their metallicities. There are eight *Century Survey* BHB stars ($|Z|$ in the range 1.5 to 3.0 kpc) with $P_{\text{halo}} < 0.60$ and $[\text{Fe}/\text{H}] < -1.50$ and if all these stars are disk stars then 10% of the *Century Survey* BHB sample could belong to the disk. To proceed further, we need more precise $[\text{Fe}/\text{H}]$ for these stars; meanwhile we suggest that 10% be regarded as an *upper limit* to the percentage of disk stars in the *Century Survey* BHB sample.

A definitive discussion of the MWTD requires accurate data and a consideration of selection biases. Morrison et al. (2008) have discussed these biases. Their local sample of stars that have $[\text{Fe}/\text{H}] < -1.0$ have well-defined metallicities and contain almost no Thick Disk stars. Their sample, however, is based on surveys at high galactic latitude, so we would expect that Thick Disk stars might be under-represented. Reddy & Lambert (2008) give abundance analyses for sixty MWTD candidates drawn from the catalogs of Ariyanto et al. (2005) and Schuster et al. (2006). These catalogs also contain kinematical selection effects and so may under-represent the Thick Disk component. Reddy & Lambert find 14 stars that might be considered MWTD and 20 that they call hybrid and which might be considered either disk or halo. They were unable to identify a conclusive abundance signature that would distinguish a MWTD star from a halo star. They note that the velocity characteristics of the MWTD may not be those of the Thick Disk. This would not be surprising if minor streams were present. The overall conclusion seems to be that the population of the MWTD is small compared with that of the Thick Disk and comparable in size to that of a hybrid population of stars that cannot be conveniently classified with present data.

5.8. Postscript on the use of Reduced Proper Motions

The referee has asked us to consider the use of reduced proper motions for separating halo from thick disk stars. Stetson (1981) used this method to pick out BHB stars from other early type stars. More recently, Rybka (2006) has shown that red clump stars can be separated from intrinsically fainter stars with 90% efficiency by this method. Following Stetson, the reduced proper motion (H_V) is defined in terms of the V magnitude and the total proper motion μ as follows:

$$H_V = V + 5 + 5 \log \mu \quad (1)$$

If D is the distance and M_V is the absolute magnitude, we have:

$$V = M_V - 5 + 5 \log D \quad (2)$$

⁶ Beers et al. (2002) considered that the local fraction (within 1 kpc) of the MWTD might be of the order of 30% to 40%.

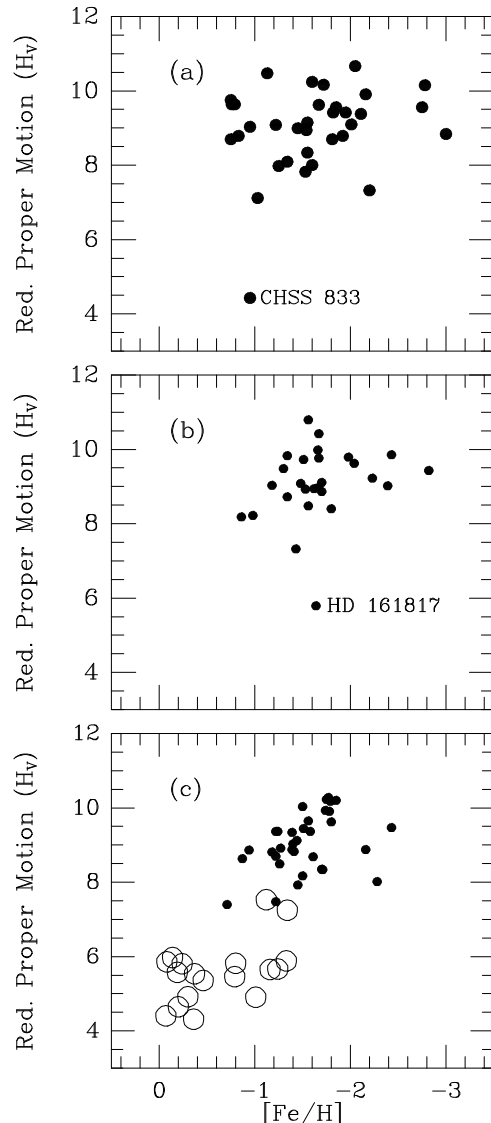


FIG. 9.— The reduced proper motion (H_V) (ordinate) vs. $[\text{Fe}/\text{H}]$ (abscissa) for (a) the nearest 34 stars ($D < 2.75$ kpc) of the *Century* CBHB sample, (b) the local BHB sample (LBHB) and (c) the RR Lyrae stars within one kpc. Here halo RR Lyrae stars are shown by filled circles and disk RR Lyrae stars by large open circles.

and so:

$$H_V = M_V + 5 \log D + 5 \log \mu \quad (3)$$

For convenience, we used equation (A3) to calculate H_V for the nearest 34 stars of the CBHB sample and we plot this against $[\text{Fe}/\text{H}]$ in Fig. 9(a). Similar plots are given in Fig. 9 (b) for the Local BHB sample and in Fig. 9 (c) for the Local RR Lyrae stars (where the disk RR Lyrae stars are shown by large open circles). We see that the reduced proper motion (H_V) affords a partial separation of the halo and disk RR Lyrae stars. HD 161817 would be considered a disk star because it has a small proper motion but a high radial velocity. Only one of CBHB sample (CHSS 833) has the H_V of a disk star which supports our conclusion that only a few percent of the *Century* BHB sample belongs to the disk.

REFERENCES

- Arifyanto, M., Fuchs. Jahreiss, H., Weilen, R. 2005, *A&A*, 433, 911
 Amrose, S., Mckay, T. 2001, *ApJL*, 560, L151
 Beers. T., Drilling, J., Rossi, S., Chiba, M. et al., 2002, *AJ*, 124, 931
 Behr, B.B. 2003, *ApJS*, 149, 101
 Brown, W.R., Beers, T.C, Wilhelm, R., Allende Prieto,C., Geller, M.J., Kenyon, S.J., Kurtz, M.J. 2008, *AJ*, 135, 564
 Cacciari, C., Corwin, T., Carney, B. 2005, *AJ*, 129, 267
 Chiba, M., Beers, T.C. 2000, *AJ*, 119, 2843
 Dambis, A.K., Rastorguev, A. 2001, *Astr. Letters*, 27, 108
 Dehnen, W., Binney, J.J. 1998, *MNRAS*, 298, 387
 ESA, 1997, *The Hipparcos and Tycho Catalogues*, ESA SP-1200, Vol. 1-17 (ESA97)
 Greenstein, J.L., Sargent, A.I. 1974, *ApJS*, 28, 1957
 Helmi. A., White, S., de Zeeuw, P.T., Zhao, H. 1999, *Nature*, 402, 53
 Hill, G., Barnes, J.V., Hilditch, R.W. 1982, *Publ. D.A.O.* 16, 111
 Hog, E., Fabricius, C., Makarov, V., Urban, S. et al. 2000, *Astron. Astrophys*, 355, L27 (Tycho-2 Catalogue)
 Ivezić. Ž., Sesar, B., Jurić, M., Bond, N. et al., 2008, *ApJ*, 684, 287
 Johnson, D.R., Soderblom, D.R. 1987, *AJ*, 93, 864
 O., Limboz, F. 2008, *astro-ph* 0809-2486
 Kpley, A. Morrison, H., Helmi, A., Kinman, T., Van Duyne, J., Martin, J., Harding, P., Norris, J., Freeman, K. 2007, *AJ*, 134, 1579
 Kinman, T.D., Castelli, F., Cacciari, C., et al. 2000, *A&A*, 364, 102
 Kinman, T.D., Cacciari, C., Bragaglia A., et al. 2007, *MNRAS*, 375, 1381
 Kinman, T.D. et al. 2008, (in preparation)
 Layden, A.C., Hanson, R.B., Hawley, S.L., Klemola, A.R., Hanley, C.J. 1996 *AJ*, 112, 2110
 Maintz, G., de Boer, K.S. 2005, *A&A*, 442, 229
 Martin, J.C., Morrison, H.L. 1998, *AJ*, 116, 1724
 Menzies, J., Cousins, A., Banfield, R., Laing, J. 1989, *SAAO Contrib.* 13, 1
 Mishenina, T., Soubiran, C., Kovtyukh, V., Korotin, S. 2004, *A&A*, 418, 551
 Monet, D., Levine, S., Casian, B. et al. 2003, *AJ*, 125, 984 (USNO-B 1.0 catalog)
 Morrison, H.L., Flynn, C., Freeman, K.C. 1990, *AJ*, 100, 1191
 Morrison, H.L., Helmi, A., Sun, J., Liu, P. et al. 2008, *astro-ph* 0804-2448
 Norris, J., Bessell, M.S., Pickles, A.J. 1985. *ApJS*, 58, 463
 Oort, J.H. 1958, *Ricerche Astronomiche*, 5, 415
 Preston, G.W., Shectman, S.A., Beers, T.C., 1991, *ApJ*, 375, 121
 Pritzl, B., Smith, H., Catelan, M., Swigart, A. 2000, *ApJ*. 530, 41
 Reddy, B., Lambert, D., Prieto, C.A. 2006, *MNRAS*, 367, 329
 Reddy, B., Lambert D. 2008, *astro-ph* 0809-0966
 Roman, N. 1955 *ApJS*, 2, 195
 Rybka, S.P. 2006, *Kinematica i Fizika Nebesnykh*, 22, 225
 Seabroke, G.M., Gilmore, G., Siebert, A. et al. 2008, *MNRAS*, 384, 11
 Schlegel, D., Finkbeiner, D. & Davis, M., 1998, *ApJ*, 500, 525
 Schuster, W., Moitinho, A., Márquez. A., Parrao, L., Covarrubias, E. 2006, *A&A*, 445, 939
 Soubiran, C., Bienaymé, O., Siebert, A. 2003, *A&A*, 398, 141
 Stetson, P., 1981, *AJ*, 86, 1337
 Stetson, P., 1991, *AJ*, 102, 1043
 Twarog, B.A., Anthony-Twarog, B.J. 1994, *AJ*, 107, 1371
 Venn, K.A., Irwin, M., Shetrone, M.D. et al., 2004, *AJ*, 128, 1177
 Zacharias N., Monet, D., Levine, Urban, S. et al. 2004a, *Bull. AAS*, 36, 1418 (Nomad Catalog)
 Zacharias N., Urban, S., Zacharias, M. Wycoff G. et al. 2004b, *AJ*, 127, 3043 (UCAC2 Catalog)

TABLE 2
DATA FOR BHB STARS WITHIN 1 KPC (SAMPLE LBHB)

HD/BD	U_{LSR}	V_{LSR}	W_{LSR}	T ^a	[Fe/H]	Z ^b	D ^c	P_{thin}^d	P_{thick}^e	P_{halo}^f
2857*	164±14	-218±17	68±10	281±24	-1.70	0.68	0.73	0.00± 0.00	0.00± 0.00	1.00± 0.00
4850	-186±19	-58±8	31±5	197 ±21	-1.18	0.54	0.57	0.00± 0.00	0.03± 0.05	0.97± 0.05
8376	-261±9	-68±17	-69±3	278±26	-2.82	0.29	0.57	0.00± 0.00	0.00± 0.00	1.00± 0.00
13780	176±17	-116±11	45±8	216±22	-1.53	0.58	0.65	0.00± 0.00	0.01± 0.01	0.99± 0.01
14829*	111±6	-188±20	154±5	267±21	-2.39	0.65	0.73	0.00± 0.00	0.00±0.00	1.00± 0.00
31943	55±7	-160±11	37±9	173±16	-0.98	0.20	0.32	0.00± 0.00	0.31± 0.04	0.69± 0.04
252940	-131±5	-176±17	63±6	228±19	-1.80	0.03	0.47	0.00± 0.00	0.00± 0.00	1.00± 0.00
60778*	47±8	-142±13	-107±12	184±19	-1.34	0.08	0.45	0.00± 0.00	0.04± 0.05	0.96± 0.05
74721*	7±4	-171±16	-98±12	197±20	-1.48	0.19	0.36	0.00± 0.00	0.03± 0.05	0.97± 0.05
78913	107±3	-311±5	23±9	330±11	-1.43	0.11	0.47	0.00± 0.00	0.00± 0.00	1.00± 0.00
86986*	259±25	-216±22	52±5	341±34	-1.66	0.21	0.28	0.00± 0.00	0.00± 0.00	1.00± 0.00
87047	38±11	-308±29	132±4	337±31	-2.43	0.52	0.65	0.00± 0.00	0.00± 0.00	1.00± 0.00
87112	94±5	-259±22	-53±8	281±24	-1.56	0.38	0.52	0.00± 0.00	0.00± 0.00	1.00± 0.00
93329	2±6	-320±23	73±11	328±26	-1.30	0.33	0.39	0.00± 0.00	0.00± 0.00	1.00± 0.00
106304	-22±8	-222±14	-166±22	278±27	-1.34	0.14	0.38	0.00± 0.00	0.00± 0.00	1.00± 0.00
+42 2309*	28±5	-189±18	-105±6	218±20	-1.62	0.88	0.91	0.00± 0.00	0.00± 0.01	1.00± 0.01
109995*	4±3	-199±18	-95±5	221±19	-1.70	0.21	0.22	0.00± 0.00	0.01± 0.01	0.99± 0.01
+25 2602*	-195±21	-213±22	-43±5	292±31	-1.98	0.72	0.72	0.00± 0.00	0.00± 0.00	1.00± 0.00
117880	52±5	-308±24	-43±15	315±29	-1.51	0.25	0.37	0.00± 0.00	0.00± 0.00	1.00± 0.00
128801	41±8	-95±10	-107±6	149±14	-1.56	0.26	0.31	0.00± 0.00	0.23± 0.10	0.77± 0.10
130095	-79±15	-246±22	75±4	269±27	-2.04	0.12	0.25	0.00± 0.00	0.00± 0.00	1.00± 0.00
130201	43±5	-104±8	-82±11	139±14	-0.86	0.15	0.68	0.00± 0.00	0.52± 0.20	0.48± 0.20
139961	-44±18	-379±32	100±8	394±38	-1.67	0.05	0.38	0.00± 0.00	0.00± 0.00	1.00± 0.00
161817*	-168±4	-285±5	-129±3	355±7	-1.64	0.08	0.19	0.00± 0.00	0.00± 0.00	1.00± 0.00
167105	125±15	-214±8	2±8	248±19	-1.66	0.17	0.38	0.00± 0.00	0.00± 0.00	1.00± 0.00
213468	-94±6	-238±26	161±5	302±27	-1.67	0.81	0.96	0.00± 0.00	0.00± 0.00	1.00± 0.00
+01 0548*	110±7	-176±19	-22±8	208±22	-2.23	0.68	0.94	0.00± 0.00	0.04± 0.03	0.96± 0.03

^a Total Space Velocity (km/s).

^b Height of star above Galactic plane (kpc).

^c Distance of star (kpc).

^d Probability that star belongs to thin disk.

^e Probability that star belongs to thick disk.

^f Probability that star belongs to the halo.

TABLE 3
DATA FOR *Century Survey STARS* (SAMPLES CBHB & CA.)

CHSS	U_{LSR}	V_{LSR}	W_{LSR}	T ^a	[Fe/H]	Z ^b	D ^c	P_{thin} ^d	P_{thick} ^e	P_{halo} ^f	Class
Sample CBHB											
3107	-028±37	-164±36	+040±26	171±58	-0.83	2.04	2.52	0.00±0.00	0.35±0.25	0.65±0.25	BHB
3110	+073±36	-183±31	+005±24	197±53	-1.55	2.13	2.65	0.00±0.00	0.11±0.04	0.89±0.04	BHB
3034	+163±25	-183±20	-043±24	249±40	-0.75	1.31	1.86	0.00±0.00	0.00±0.00	1.00±0.00	BHB
3048	-131±28	-458±36	-164±30	504±55	-2.05	1.76	2.62	0.00±0.00	0.00±0.00	1.00±0.00	BHB
3052	+074±63	-216±49	+013±53	229±96	-1.03	1.74	2.75	0.00±0.00	0.01±0.00	0.99±0.00	BHB
3276	-082±64	-287±52	+107±49	317±96	-2.01	1.79	2.66	0.00±0.00	0.00±0.00	1.00±0.00	BHB
3218	-151±32	-242±30	-053±18	290±47	-1.67	2.12	2.63	0.00±0.00	0.00±0.00	1.00±0.00	BHB
3335	-046±27	-360±34	-023±23	364±49	-2.16	1.72	2.42	0.00±0.00	0.00±0.00	1.00±0.00	BHB
3411	+046±17	-295±24	+099±15	315±33	-3.00	1.58	2.57	0.00±0.00	0.00±0.00	1.00±0.00	BHB
3877	-335±45	-150±40	+016±22	367±64	-1.60	2.31	2.59	0.00±0.00	0.00±0.00	1.00±0.00	BHB
3886	+309±29	-217±32	+093±19	387±47	-2.75	2.42	2.68	0.00±0.00	0.00±0.00	1.00±0.00	BHB
3689	+022±42	-116±47	-034±28	123±69	-1.25	1.90	2.32	0.00±0.04	0.87±0.34	0.13±0.38	BHB
3888	-169±28	-356±44	-053±16	398±55	-2.78	2.41	2.67	0.00±0.00	0.00±0.00	1.00±0.00	BHB
3528	+116±15	-288±30	+027±19	312±39	-0.79	1.42	2.11	0.00±0.00	0.00±0.00	1.00±0.00	BHB
1676	-116±17	-204±27	-006±16	235±36	-1.45	2.00	2.74	0.00±0.00	0.01±0.03	0.99±0.03	BHB
4003	+152±65	-174±95	+112±76	257±138	-1.55	1.62	2.67	0.00±0.00	0.00±0.00	1.00±0.00	BHB
1786	+065±23	-182±30	+056±13	201±40	-0.95	2.27	2.50	0.00±0.00	0.05±0.02	0.95±0.02	BHB
1851	-036±36	-121±30	+045±18	134±50	-2.20	2.47	2.73	0.00±0.00	0.77±0.26	0.23±0.26	BHB
1930	+026±09	-252±29	+030±11	255±32	-1.82	2.15	2.27	0.00±0.00	0.00±0.00	1.00±0.00	BHB
0833	+049±11	+002±16	-052±10	071±22	-0.95	2.50	2.57	0.33±0.21	0.65±0.19	0.02±0.01	BHB
2181	-222±40	-166±31	-006±17	277±53	-1.85	2.30	2.72	0.00±0.00	0.00±0.00	1.00±0.00	BHB
2183	-114±15	-352±36	+104±12	384±41	-1.72	2.64	2.68	0.00±0.00	0.00±0.00	1.00±0.00	BHB
2233	+063±25	-119±26	-026±12	137±38	-1.34	2.29	2.36	0.00±0.00	0.77±0.13	0.23±0.13	BHB
2305	-129±17	-122±17	+082±10	196±26	-1.81	2.28	2.30	0.00±0.00	0.02±0.02	0.98±0.02	BHB
2366	+288±48	-286±41	-093±42	416±76	-1.92	1.77	2.70	0.00±0.00	0.00±0.00	1.00±0.00	BHB
2522	-222±42	-077±31	+081±10	249±53	-0.76	1.55	2.32	0.00±0.00	0.00±0.00	1.00±0.00	BHB
2523	+099±11	-265±23	+018±14	283±29	-1.95	2.28	2.48	0.00±0.00	0.00±0.00	1.00±0.00	BHB
2607	+094±36	-240±33	+028±31	259±58	-1.54	1.89	2.63	0.00±0.00	0.00±0.00	1.00±0.00	BHB
2934	-070±21	-341±22	-008±24	348±39	-2.11	1.48	2.42	0.00±0.00	0.00±0.00	1.00±0.00	BHB
3075	+024±26	-164±20	-072±18	181±37	-0.75	1.85	2.46	0.00±0.00	0.14±0.17	0.86±0.17	BHB
3083	+072±32	-429±37	-054±30	438±57	-1.13	1.85	2.37	0.00±0.00	0.00±0.00	1.00±0.00	BHB
3096	-095±29	-192±21	+083±17	230±40	-1.22	1.52	2.09	0.00±0.00	0.00±0.00	1.00±0.00	BHB
3100	-116±44	-144±35	-017±27	186±62	-1.60	2.01	2.53	0.00±0.00	0.14±0.40	0.86±0.40	BHB
2996	+023±24	-162±19	-014±22	164±38	-1.53	1.72	2.73	0.00±0.00	0.51±0.22	0.49±0.22	BHB
3019	-017±14	-259±15	+001±14	260±25	-1.92	1.72	2.93	0.00±0.00	0.00±0.00	1.00±0.00	BHB
3029	+153±34	-037±21	-013±20	158±45	-1.24	1.72	2.76	0.20±0.02	0.31±0.28	0.49±0.27	BHB
3041	+130±33	-185±28	-140±30	266±53	-2.07	2.01	2.92	0.00±0.00	0.00±0.00	1.00±0.00	BHB
3799	+059±101	-231±96	+037±41	241±145	-1.25	2.76	2.98	0.00±0.00	0.00±0.00	1.00±0.00	BHB
1626	+126±74	-167±67	+032±35	212±106	-1.00	2.61	2.94	0.00±0.00	0.02±0.00	0.98±0.00	BHB
3803	-022±91	-284±94	-190±37	342±136	-2.06	2.75	2.93	0.00±0.00	0.00±0.00	1.00±0.00	BHB
3294	+135±71	-105±61	-018±53	172±108	-1.25	2.01	2.76	0.00±0.00	0.24±0.03	0.76±0.03	BHB
3299	-110±32	-127±30	-083±29	187±53	-1.36	1.86	2.90	0.00±0.00	0.05±0.32	0.95±0.32	BHB
1641	-010±23	-130±26	+047±12	139±37	-1.47	2.57	2.90	0.00±0.00	0.73±0.19	0.27±0.19	BHB
3383	-017±22	-090±24	-032±20	097±38	-0.74	1.93	2.84	0.00±0.05	0.94±0.07	0.06±0.12	BHB
3395	-169±28	-328±38	-052±22	373±52	-2.03	1.91	2.86	0.00±0.00	0.00±0.00	1.00±0.00	BHB
3416	+148±69	-044±75	-059±69	165±123	-1.81	1.78	2.93	0.00±0.00	0.19±0.00	0.81±0.00	BHB
3880	-129±39	-381±55	-085±23	411±071	-1.61	2.56	2.93	0.00±0.00	0.00±0.00	1.00±0.00	BHB
1652	-042±73	-325±85	+002±45	328±121	-1.46	2.51	2.99	0.00±0.00	0.00±0.00	1.00±0.00	BHB
3535	+066±62	-265±86	-061±63	280±123	-0.62	2.02	2.92	0.00±0.00	0.00±0.01	1.00±0.01	BHB
3927	-320±34	-346±47	-056±28	475±064	-2.14	2.34	2.95	0.00±0.00	0.00±0.00	1.00±0.00	BHB
3638	+066±28	-305±49	+047±34	316±066	-2.20	1.82	2.92	0.00±0.00	0.00±0.00	1.00±0.00	BHB
1699	+014±26	+058±26	-011±26	061±045	-1.99	1.70	2.90	0.60±0.20	0.39±0.19	0.01±0.01	BHB
1717	-007±15	-512±38	-029±15	513±044	-2.24	2.44	2.80	0.00±0.00	0.00±0.00	1.00±0.00	BHB
0045	+045±37	-098±54	+020±20	110±068	-1.61	2.59	2.93	0.00±0.07	0.92±0.07	0.08±0.14	BHB
0786	+141±17	-317±31	+034±10	349±037	-1.68	2.55	2.86	0.00±0.00	0.00±0.00	1.00±0.00	BHB
1830	-214±17	-227±25	+091±12	325±033	-2.02	2.53	2.77	0.00±0.00	0.00±0.00	1.00±0.00	BHB
1955	+015±30	-065±31	+113±26	131±050	-0.68	2.01	2.81	0.00±0.00	0.37±0.25	0.63±0.25	BHB
1982	-136±62	-116±61	-046±23	185±090	-1.58	2.67	2.83	0.00±0.08	0.09±0.40	0.91±0.47	BHB
2078	-235±77	-125±73	+107±58	287±121	-1.87	2.12	2.92	0.00±0.00	0.00±0.00	1.00±0.00	BHB
0196	-067±12	-143±18	+093±10	183±024	-1.63	2.79	2.86	0.00±0.00	0.06±0.02	0.94±0.02	BHB
2103	-139±52	-215±53	+039±15	259±076	-1.80	2.79	2.85	0.00±0.00	0.00±0.04	1.00±0.04	BHB
2122	-006±22	-211±25	+059±13	219±036	-2.28	2.72	2.90	0.00±0.00	0.02±0.02	0.98±0.02	BHB
2152	-132±43	-179±44	+045±13	227±063	-1.68	2.85	2.90	0.00±0.00	0.01±0.10	0.99±0.10	BHB
2161	+043±28	-411±37	+316±12	520±048	-1.17	2.84	2.90	0.00±0.00	0.00±0.00	1.00±0.00	BHB
2323	-124±27	-239±37	-031±10	271±047	-0.98	2.93	2.93	0.00±0.00	0.00±0.01	1.00±0.01	BHB
2349	-114±21	-467±51	+094±10	490±056	-1.92	2.95	2.96	0.00±0.00	0.00±0.00	1.00±0.00	BHB
2353	-004±54	-037±54	+160±11	164±077	-1.99	2.94	2.95	0.00±0.00	0.01±0.00	0.99±0.00	BHB
2372	+129±17	-184±19	-092±10	243±027	-1.49	2.95	2.95	0.00±0.00	0.00±0.00	1.00±0.00	BHB
2376	-138±16	-022±15	+116±12	182±025	-1.67	2.23	2.91	0.00±0.00	0.02±0.00	0.98±0.00	BHB
2436	+216±20	-177±20	-094±12	295±031	-1.43	2.77	2.88	0.00±0.00	0.00±0.00	1.00±0.00	BHB
2441	-168±52	-041±38	-050±15	180±066	-1.95	2.71	2.98	0.01±0.25	0.09±0.20	0.90±0.45	BHB
2541	-158±20	-167±18	-005±11	230±029	-1.61	2.76	2.96	0.00±0.00	0.00±0.02	1.00±0.02	BHB
2585	+023±51	-329±48	-062±34	336±078	-1.59	2.23	2.76	0.00±0.00	0.00±0.00	1.00±0.00	BHB

TABLE 3 — *Continued*

CHSS	U_{LSR}	V_{LSR}	W_{LSR}	T ^a	[Fe/H]	[Z]	D ^c	P_{thin} ^d	P_{thick} ^e	P_{halo} ^f	Class
1423	-160±65	-166±60	+177±29	291±093	-1.60	2.62	2.91	0.00±0.00	0.00±0.00	1.00±0.00	BHB
2713	+007±50	-324±48	+219±36	391±078	-2.72	2.24	2.80	0.00±0.00	0.00±0.00	1.00±0.00	BHB
2739	-044±26	-150±24	+165±25	227±043	-1.55	1.86	2.81	0.00±0.00	0.00±0.00	1.00±0.00	BHB
2758	+167±17	-240±14	-096±13	308±026	-1.88	2.10	2.80	0.00±0.00	0.00±0.00	1.00±0.00	BHB
2793	+077±39	-291±25	-039±24	304±052	-1.60	2.10	2.89	0.00±0.00	0.00±0.00	1.00±0.00	BHB
3077	-107±82	-166±58	+050±58	204±116	-2.02	2.07	2.94	0.00±0.00	0.04±0.08	0.96±0.08	BHB
3139	+051±26	-151±23	-014±18	160±039	-1.50	2.27	2.77	0.00±0.00	0.55±0.18	0.45±0.18	BHB
1618	+049±24	-426±30	+059±18	433±042	-1.81	2.53	2.95	0.00±0.00	0.00±0.00	1.00±0.00	BHB
2991	+114±31	-121±23	+016±24	167±045	-1.42	2.00	2.87	0.00±0.00	0.34±0.14	0.66±0.14	BHB
Sample CA											
3148	+084±19	-016±16	+055±14	102±29	-0.86	1.12	1.27	0.17±0.10	0.75±0.02	0.08±0.13	A
3028	-029±39	-091±32	-089±33	131±60	-0.56	0.94	1.44	0.00±0.01	0.58±0.46	0.42±0.47	A
3033	+047±13	-021±11	-046±11	069±20	-1.60	0.86	1.25	0.30±0.24	0.68±0.22	0.02±0.01	A
3046	+100±18	-031±12	-010±11	105±24	-0.28	1.11	1.75	0.54±0.17	0.42±0.17	0.04±0.01	A
1628	+019±48	-072±45	-043±23	086±70	+0.19	1.75	1.96	0.01±0.28	0.94±0.10	0.05±0.19	A
3216	+129±38	-135±36	-077±26	202±58	+0.00	1.46	1.74	0.00±0.00	0.02±0.01	0.98±0.01	A
3358	+024±09	+012±10	+001±11	027±17	-1.28	0.64	1.11	0.85±0.00	0.15±0.00	0.00±0.00	A
3180	+126±34	-035±31	-024±22	133±51	-1.10	1.11	1.28	0.31±0.23	0.51±0.30	0.18±0.07	A
3361	+039±09	-039±10	-019±11	058±17	+0.00	1.12	1.80	0.43±0.22	0.56±0.21	0.01±0.01	A
3867	+118±44	-140±47	-035±23	186±68	-1.49	1.14	1.23	0.00±0.00	0.12±0.02	0.88±0.02	A
3379	+059±31	-014±32	+043±30	074±54	-0.25	0.95	1.51	0.40±0.16	0.58±0.05	0.02±0.11	A
3382	-036±12	-011±12	-012±10	040±20	-0.31	1.00	1.50	0.77±0.11	0.23±0.11	0.00±0.00	A
3384	+076±11	+005±11	+034±11	083±19	-1.21	0.75	1.21	0.63±0.14	0.35±0.12	0.02±0.02	A
3394	-028±14	-025±14	+008±13	038±24	-1.26	0.63	1.09	0.68±0.11	0.32±0.11	0.00±0.00	A
3272	+129±20	-038±20	+041±17	141±33	-0.57	1.07	1.42	0.11±0.03	0.54±0.25	0.35±0.28	A
3438	+083±13	-084±20	+018±22	119±32	-0.11	1.02	1.70	0.01±0.01	0.86±0.03	0.13±0.02	A
3455	+136±41	-008±50	-058±46	148±79	+0.00	1.06	1.80	0.07±0.07	0.41±0.03	0.52±0.05	A
3904	+151±23	+012±23	+050±17	160±37	-0.40	1.22	1.46	0.11±0.22	0.28±0.18	0.61±0.40	A
3468	+040±13	+013±15	-009±14	043±24	-0.21	0.93	1.57	0.83±0.03	0.17±0.03	0.00±0.00	A
3916	+264±22	-244±35	+128±20	382±46	-1.01	1.05	1.31	0.00±0.00	0.00±0.00	1.00±0.00	A
3474	+046±26	-073±35	+053±30	101±53	-1.04	0.72	1.20	0.01±0.00	0.91±0.10	0.09±0.10	A
3920	-165±38	-067±45	-052±28	186±65	+0.00	1.38	1.68	0.00±0.23	0.06±0.20	0.94±0.42	A
3561	-020±14	-022±13	-026±13	039±23	-1.29	0.74	1.13	0.60±0.26	0.40±0.25	0.00±0.01	A
3564	+015±19	+016±22	-010±19	024±35	+0.00	1.15	1.67	0.84±0.05	0.16±0.05	0.00±0.00	A
1674	+054±31	-036±40	-085±28	107±58	-0.88	1.14	1.56	0.00±0.10	0.80±0.22	0.20±0.33	A
3661	-218±34	-438±70	-001±39	489±87	+0.00	1.16	1.83	0.00±0.00	0.00±0.00	1.00±0.00	A
3665	+057±31	-081±49	-052±39	112±70	-0.07	1.01	1.65	0.00±0.26	0.87±0.12	0.13±0.39	A
3951	+029±19	+050±21	+009±16	058±33	+0.00	1.31	1.82	0.69±0.26	0.31±0.25	0.00±0.01	A
3960	+197±24	-108±28	-009±21	225±42	-0.10	1.21	1.69	0.00±0.00	0.00±0.00	1.00±0.00	A
3758	-116±24	+000±33	+022±29	118±50	-1.06	0.81	1.31	0.68±0.04	0.28±0.14	0.04±0.09	A
3992	-035±18	-066±23	+000±19	075±35	-0.38	0.94	1.52	0.11±0.18	0.87±0.15	0.02±0.03	A
4009	+109±38	-040±54	-056±47	129±81	-0.10	0.89	1.54	0.04±0.32	0.68±0.03	0.28±0.34	A
4013	+047±20	-047±25	-006±22	067±39	+0.00	1.09	1.82	0.36±0.31	0.63±0.30	0.01±0.01	A
1784	+004±22	+070±23	+038±13	080±34	-0.17	1.43	1.57	0.19±0.30	0.79±0.27	0.02±0.03	A
1859	+082±14	-114±18	+044±10	147±25	-0.30	1.57	1.68	0.00±0.00	0.59±0.02	0.41±0.02	A
1927	-163±21	+016±22	-043±24	169±39	+0.38	1.24	1.90	0.12±0.25	0.18±0.13	0.70±0.38	A
2050	-087±17	-009±12	+022±10	090±23	-0.32	1.50	1.68	0.69±0.01	0.30±0.00	0.01±0.01	A
2084	-039±38	-039±35	+040±19	068±55	-0.95	1.20	1.31	0.21±0.08	0.77±0.05	0.02±0.04	A
2158	+061±08	+031±07	+021±10	072±15	-1.63	1.21	1.24	0.74±0.11	0.25±0.10	0.01±0.01	A
2204	-075±11	-042±07	+159±10	181±16	+0.00	1.72	1.74	0.00±0.00	0.00±0.00	1.00±0.00	A
2206	+087±14	+021±14	+040±15	098±25	+0.00	1.27	1.67	0.53±0.28	0.44±0.21	0.03±0.07	A
2258	-010±16	-127±23	-040±12	134±30	-0.42	1.57	1.60	0.00±0.00	0.79±0.26	0.21±0.26	A
2435	+078±10	-022±07	+050±09	095±15	-1.35	1.23	1.26	0.21±0.08	0.74±0.04	0.06±0.05	A
2579	-074±20	+008±16	+045±14	087±29	-1.46	1.02	1.23	0.46±0.20	0.52±0.19	0.02±0.01	A
2868	+018±27	+053±10	-006±11	056±31	-0.39	0.89	1.44	0.68±0.09	0.32±0.09	0.00±0.00	A
2886	-015±08	-020±09	-018±08	031±14	-0.32	0.91	1.57	0.68±0.13	0.32±0.13	0.00±0.00	A
2893	+015±17	-006±12	-002±14	016±25	-0.93	0.86	1.47	0.82±0.06	0.18±0.05	0.00±0.00	A
2908	+005±31	-014±21	+059±26	061±46	-0.53	0.71	1.18	0.16±0.17	0.82±0.11	0.02±0.06	A
3080	+008±13	-084±19	-141±19	164±30	+0.00	1.22	1.68	0.00±0.00	0.03±0.09	0.97±0.09	A
3103	-010±12	-018±12	-022±11	030±20	-0.55	1.09	1.43	0.67±0.19	0.33±0.19	0.00±0.00	A

^a Total Space Velocity (km/s).^b Height of star above Galactic plane (kpc).^c Distance of star (kpc).^d Probability that star belongs to thin disk.^e Probability that star belongs to thick disk.^f Probability that star belongs to the halo.